

**ORIGINAL ARTICLE**

# Population pharmacokinetic modelling of busulfan and the influence of body composition in paediatric Fanconi anaemia patients

Matthijs W. van Hoogdalem<sup>1</sup>  | Chie Emoto<sup>1,3</sup>  | Tsuyoshi Fukuda<sup>1,3</sup>  |  
Tomoyuki Mizuno<sup>1,3</sup>  | Parinda A. Mehta<sup>2,3</sup> | Alexander A. Vinks<sup>1,3</sup> 

<sup>1</sup>Division of Clinical Pharmacology, Cincinnati Children's Hospital Medical Center, Cincinnati, OH, USA

<sup>2</sup>Division of Bone Marrow Transplantation and Immune Deficiency, Cincinnati Children's Hospital Medical Center, Cincinnati, OH, USA

<sup>3</sup>Department of Pediatrics, University of Cincinnati College of Medicine, Cincinnati, OH, USA

**Correspondence**

Alexander A. Vinks, Division of Clinical Pharmacology, Cincinnati Children's Hospital Medical Center, 3333 Burnet Ave, MLC 6018, Cincinnati, OH, USA  
Email: sander.vinks@cchmc.org

**Aims:** Fanconi anaemia (FA) is a rare disorder characterized by progressive bone marrow failure that requires haematopoietic cell transplantation (HCT). Busulfan is used in conditioning regimens prior to HCT. Doses used in non-FA patients cause life-threatening toxicities in FA patients and data on busulfan pharmacokinetics (PK) in this population are limited. This study characterized busulfan PK in paediatric FA patients using population PK modelling and evaluated the effect of body composition on steady-state concentrations ( $C_{ss}$ ).

**Methods:** A total of 200 busulfan plasma concentrations in 29 FA patients from a recent study (Clinicaltrials.gov; NCT01082133) were available for population PK modelling. The effect of different body size-scaled doses and body compositions on  $C_{ss}$  was investigated using population PK modelling.

**Results:** Fat free mass (FFM) was identified as the best size descriptor in a two-compartment busulfan PK model in FA patients. Conventional dosing, based on an amount of busulfan per kilogram of total body mass, resulted in higher  $C_{ss}$  in FA patients with higher body mass index (BMI). A newly proposed FFM-based dosing strategy would eliminate the observed trend of higher concentrations in high BMI patients, and achieve consistent  $C_{ss}$  across a wide BMI spectrum.

**Conclusions:** This is the first study to describe the population PK of busulfan in paediatric FA patients. The proposed model will facilitate PK model-informed precision dosing. FFM-based dosing is expected to improve the probability of achieving target  $C_{ss}$ , particularly in obese patients, while minimizing the risk of overdosing.

**KEYWORDS**

busulfan, Fanconi anaemia, paediatrics, population pharmacokinetic modelling

The authors confirm that the Principal Investigator for this study was Dr Parinda A. Mehta, who had full clinical responsibility for the patients participating in the study.

This is an open access article under the terms of the Creative Commons Attribution-NonCommercial License, which permits use, distribution and reproduction in any medium, provided the original work is properly cited and is not used for commercial purposes.

© 2019 The Authors. British Journal of Clinical Pharmacology published by John Wiley & Sons Ltd on behalf of British Pharmacological Society

## 1 | INTRODUCTION

Fanconi anaemia (FA) is a rare inherited genetically and phenotypically heterogeneous disorder that causes progressive bone marrow failure.<sup>1</sup> FA patients are predisposed to developing leukaemia and solid tumours. Median life expectancy is therefore 23 years.<sup>2</sup> Hence, it affects mostly paediatric patients. Various congenital malformations are often seen, including short stature and kidney abnormalities associated with decreased renal function.<sup>2</sup> These anatomical and physiological characteristics might influence drug behaviour in FA patients, therefore understanding the differences in drug disposition compared to non-FA patients is of clinical importance.

Allogeneic haematopoietic cell transplantation (HCT) is an effective therapy to treat the haematological complications of patients with FA.<sup>3</sup> Busulfan is widely used in conditioning regimens prior to HCT for various haematological disorders. Due to large variability in busulfan pharmacokinetics (PK) in combination with its narrow therapeutic index, monitoring of busulfan concentration is recommended to maximize the effect while minimizing the incidence of side effects. High systemic exposure to busulfan is correlated with toxicities such as sinusoidal obstruction syndrome and acute graft-versus-host disease in adult patients undergoing HCT.<sup>4,5</sup> In contrast, low exposure is associated with an increased risk of graft rejection and relapse.<sup>6,7</sup> Toxicities emerging from conditioning regimens are more common in FA patients due to their high chemotherapy sensitivity, which is related to an inability to repair DNA damage.<sup>8,9</sup> Finding the right dose in FA patients has been a challenge for clinicians, in part due to limited information on the PK of busulfan in this patient population.

Busulfan PK has been recently described in FA patients.<sup>10</sup> The aim of this study was to characterize the population PK of busulfan in paediatric patients with FA. The effects of differences in body size on busulfan PK in FA patients were specifically examined, since body weight has been reported to be an important predictive covariate in non-FA patients<sup>10-19</sup> and the FA patient population shows a unique physical characteristic with wide body weight distribution. That is, in general FA patients are of notably short stature and underweight compared to a relatively healthy paediatric population,<sup>2</sup> but overweight and obesity can still occur.

## 2 | METHODS

### 2.1 | Patients and study design

Data from a subset of patients who participated in a recent phase 2 study (ClinicalTrials.gov: NCT01082133) by Mehta *et al.* were used for the development of the population PK model.<sup>20</sup> The Institutional Review Boards of Cincinnati Children's Hospital Medical Center approved the study and all parents/guardians and/or patients provided written informed consent and assent before enrolment in the study. In brief, in the clinical study, two groups of patients received either an initial busulfan dose of 0.8 or 1 mg kg<sup>-1</sup> (based on patient age and weight as previously reported<sup>11,13</sup>), or a reduced dose of 0.6

#### What is already known about this subject

- Busulfan has a narrow therapeutic index and is used in preparative regimens prior to haematopoietic cell transplantation in the rare disorder Fanconi anaemia (FA).
- Total body mass-based dosing is currently recommended in patients with FA.
- Body size is a predictive covariate for busulfan pharmacokinetics (PK) in non-FA paediatric patients.

#### What this study adds

- This is the first study describing population PK of busulfan in paediatric FA patients.
- Size-normalized busulfan PK in FA patients was similar to that as in non-FA patients.
- Fat free mass-based dosing is expected to improve target steady-state concentration attainment, particularly in obese patients, which would reduce variability in clinical outcomes.

or 0.8 mg kg<sup>-1</sup> as a 2-hour intravenous infusion. Blood samples were collected at 0, 15 and 30 minutes, and 1.5, 2, 3 and 4 hours after the end of intravenous infusion of busulfan. Based on the PK results, subsequent busulfan doses were reduced (if necessary).<sup>20</sup> A total of 200 busulfan plasma concentrations from 29 FA patients after first dose were available for PK analysis. Busulfan concentrations were measured by gas chromatography with mass spectrometry detection as previously described.<sup>21</sup> The within- and between-day coefficients of variation for the assay were below 8%. The dynamic range of the assay was from 125 to 7500 ng mL<sup>-1</sup> with a lower limit of quantification of 125 ng mL<sup>-1</sup>. Patients' demographic data and clinical laboratory test results were collected as part of routine clinical care.

### 2.2 | Population PK modelling

Population PK analysis was performed by nonlinear mixed effect modelling using NONMEM (version 7.2, ICON, Gaithersburg, MD, USA), with PDx-POP version 5.0 (ICON) and Pirana version 2.7.1 (Pirana Software & Consulting BV, <http://pirana-software.com>) as interfaces. First-order conditional estimation with interaction (FOCE-I) was applied for all runs. Both one and two-compartment models were explored, and model selection was based on goodness-of-fit diagnostics plots, comparisons based on the minimum objective function value (OFV) and evaluation of the estimates of population fixed and random effect parameters. Interindividual variability was assessed using the following model (Equation (1)):

$$\theta_i = \theta_{TV} \cdot \exp(\eta_i) \quad (1)$$

where  $\theta_i$  is the estimated parameter value for individual  $i$ ,  $\theta_{TV}$  is the typical value of parameter  $\theta$  in the structural model, and  $\eta_i$  is an inter-individual random effect for individual  $i$ , which was assumed to follow a normal distribution with a mean of 0 and a variance of  $\omega^2$ . Investigated PK parameters were clearance (CL), volume of distribution of the central compartment ( $V_1$ ), intercompartmental clearance (Q), and volume of distribution of the peripheral compartment ( $V_2$ ). A proportional error model and a combined proportional and additive error model were explored to describe the residual error.

Both allometric and linear scaling were examined to account for differences in body size and composition as follows (Equation (2)):

$$\theta_i = \theta_{TV} \times \left( \frac{BM_i}{BM_{std}} \right)^{power} \quad (2)$$

where  $BM_i$  is the size descriptor for body mass (ie, total body mass [TBM], fat free mass [FFM], normal fat mass [NFM], ideal body mass [IBM], or body mass index [BMI]) for individual  $i$ ,  $BM_{std}$  is the value for the size descriptor in a standard adult male, and power is the allometric exponent or equals 1 in linear scaling.

Lean body weight (LBW) and FFM are often used interchangeably in clinical practice to account for body composition differences. In this study, FFM was used since the LBW formula has been reported to lead to some inconsistencies in the prediction of LBW at extremes of height and weight.<sup>22-24</sup> FFM was predicted for males and females using the following equations (Equations (3) and (4), respectively):

$$FFM_{male} = \left( 0.88 + \left( \frac{1 - 0.88}{1 + \left( \frac{age_i}{13.4} \right)^{-12.7}} \right) \right) \times \left( \frac{42.92 \times HT_i^2 \times TBM_i}{30.93 \times HT_i^2 + TBM_i} \right) \quad (3)$$

$$FFM_{female} = \left( 1.11 + \left( \frac{1 - 1.11}{1 + \left( \frac{age_i}{7.1} \right)^{-1.1}} \right) \right) \times \left( \frac{37.99 \times HT_i^2 \times TBM_i}{35.98 \times HT_i^2 + TBM_i} \right) \quad (4)$$

where  $age_i$  is the age of individual  $i$  in years,  $HT_i$  is height of individual  $i$  in metres (m) and  $TBM_i$  is the total body mass of individual  $i$  in kilograms (kg).<sup>24,25</sup> The lower bounds ( $\alpha$ ) of the sigmoid hyperbolic models for males and females, are 0.88 and 1.11, respectively, and 1 in the numerators is the upper bound ( $\beta$ ). The FFM maturation half-times are 13.4 and 7.1, the sigmoidicity coefficients ( $\gamma$ ) are 12.7 and 1.1, the maximum FFM values for any given height ( $WHS_{max}$ ) are 42.92 and 37.99, and the values for TBM when FFM is half of  $WHS_{max}$  are 30.93 and 35.98 for males and females, respectively.<sup>22,25</sup>

In this study, NFM was also assessed as a size descriptor according to previous reports.<sup>17</sup> FFM was used to calculate NFM as follows (Equation (5)):

$$NFM = FFM + Ffat \times (TBM - FFM) \quad (5)$$

where  $Ffat$  is a fraction that reflects the role of fat (TBM minus FFM) on metabolic processes or physiological volumes.<sup>22</sup> If  $Ffat$  is 0, size is completely described by FFM, whereas if  $Ffat$  is 1, TBM describes the body size mass entirely.

Lastly, IBM was tested as a size descriptor, which has been suggested as a dosing mass index for several drugs in obese children.<sup>26</sup> IBM was calculated as follows (Equation (6)):

$$IBM = 2.396 e^{0.01863 \times HT_i} \quad (6)$$

where IBM is in kilograms and  $HT_i$  is the height of individual  $i$  in centimetres (cm).<sup>27</sup> If the height of the patient exceeded 5 feet (154 cm), the IBM for males and females was calculated using the following formulas (Equation (7) and (8), respectively)<sup>28</sup>:

$$IBM_{male} = 50 \text{ kg} + 2.3 \text{ kg for each inch over 5 feet} \quad (7)$$

$$IBM_{female} = 45.5 \text{ kg} + 2.3 \text{ kg for each inch over 5 feet} \quad (8)$$

Potential covariates (ie, age, height, body surface area, BMI, TBM, FFM, NFM, IBM, nuclear glomerular filtration rate (GFR), serum creatinine, serum albumin, serum aspartate transaminase (AST), serum alanine transaminase (ALT) and gender) were plotted individually against the post hoc Bayesian individual PK parameter estimates, and were examined as a covariate based on their visual correlation. In addition, covariates were identified by calculating the difference in minimum OFV between models with and without the covariate relationship and on the basis of their studied or theoretical relationship with busulfan PK. The differences in OFVs from nested models was assumed to be  $\chi^2$  distributed. A drop of more than 6.63 points ( $P < 0.01$ ) was considered to be significant.

### 2.3 | Model evaluation

To evaluate the models and to identify potential bias due to model misspecification, the following diagnostic plots were used: observed value (DV) vs population-predicted value (PRED), DV vs individual-predicted value (IPRED), conditional weighted residuals (CWRES) vs PRED and CWRES vs time after start of the infusion. Non-parametric bootstrap analysis was run with 1000 resampled datasets.<sup>29</sup> The estimated medians and 95% confidence intervals were compared with the final model estimates. For the validation of the final model, the prediction-corrected visual predictive check (pcVPC) was used by simulating 1000 datasets.<sup>30</sup> The observations were compared with the distribution of the simulated concentrations.

### 2.4 | Individual steady-state concentration estimates by Bayesian estimation

Patient demographics, dosing information and busulfan plasma concentration-time data were used to estimate individual PK parameters by using the MwPharm++ software (version 1.5.1, MEDIWARE, Inc., Prague, Czech Republic), a therapeutic drug management application. In the application, the final population PK model parameters were used as prior population information for Bayesian estimation

using individually observed concentrations as feedback. The workflow of this analysis is depicted in Figure S1. In this study, busulfan exposure was reflected as concentration at steady-state ( $C_{ss}$ ).  $C_{ss}$  was calculated using the following formula (Equation (9))<sup>31</sup>:

$$C_{ss} = \frac{AUC_{0-\infty}}{\tau} \quad (9)$$

where  $AUC_{0-\infty}$  is the area under the curve from  $t = 0$  to infinity and  $\tau$  is the dosing interval.

The target  $C_{ss}$  has been suggested as  $0.616 \text{ mg L}^{-1} \leq C_{ss} < 1.026 \text{ mg L}^{-1}$  by Booth *et al.* in non-FA paediatric patients based on a 6-hour dosing interval attained by dosing per TBM.<sup>13</sup> Due to high chemotherapy sensitivity in FA, Mehta *et al.* aimed at a significantly lower exposure of  $\leq 0.35 \text{ mg L}^{-1}$  by 12-hour

dosing intervals.<sup>20</sup> The subset of patients whose data were used in this PK analysis received either a busulfan dose of  $0.8 \text{ mg kg}^{-1}$  TBM or a lowered dose of  $0.6 \text{ mg kg}^{-1}$  TBM.  $C_{ss}$  was calculated following this initial dose. To eliminate as a possible confounder that the patients' body compositions (eg, overweight, obesity) were not equally distributed in the two dosing arms,  $C_{ss}$  was estimated using individual PK parameters for the scenario in which all patients received the same simulated dose (ie, 0.6, 0.8, 1.0 and  $1.2 \text{ mg kg}^{-1}$  TBM). This dosing scenario allowed assessment of the effect of different body compositions on the  $C_{ss}$  estimate. In addition, in order to account for redundant fat mass that might not contribute to busulfan PK,  $C_{ss}$  was estimated following simulated FFM-based doses (ie, 0.6, 0.8, 1.0 and  $1.2 \text{ mg kg}^{-1}$  FFM).

## 2.5 | Statistical analysis

The correlation between a patient's BMI and the estimated busulfan  $C_{ss}$  was assessed based on linear regression analysis using GraphPad Prism (version 7.0, GraphPad Software, Inc., San Diego, CA, USA). Differences in estimated  $C_{ss}$  achieved between patient subpopulations were analysed by the nonparametric Mann-Whitney  $U$ -test.

**TABLE 1** Demographic information and clinical laboratory test results of patients at enrolment in this study

|   | Median (95% CI, $n = 29$ ) |
|---|----------------------------|
| Age (years)   | 8.0 (6.3-10.6)             |
| Weight (kg)   | 19.9 (15.9-33.0)           |
| Height (cm)   | 120.6 (107.1-133.2)        |
| Body mass index (BMI, $\text{kg m}^{-2}$ )  | 16.0 (13.8-18.1)           |
| Initial dose ( $\text{mg } 12 \text{ h}^{-1}$ )                                     | 13.6 (11.0-25.0)           |
| Nuclear glomerular filtration rate (GFR, $\text{ml min}^{-1} 1.73 \text{ m}^{-2}$ ) | 112 (92-129)               |
| Serum creatinine ( $\text{mg dL}^{-1}$ )  | 0.43 (0.40-0.50)           |
| Serum albumin ( $\text{g dL}^{-1}$ )  | 3.7 (3.5-4.0)              |
| Serum aspartate transaminase (AST, units $\text{L}^{-1}$ )                          | 36 (32-43)                 |
| Serum alanine transaminase (ALT, units $\text{L}^{-1}$ )                            | 32 (25-52)                 |
| Sex: male/female  | 13/16                      |

95% CI = 95% confidence interval

## 3 | RESULTS

### 3.1 | Patients

The demographic characteristics of the patients with FA are summarized in Table 1. Frequency histograms of the data are presented in Figure S2. The median age in the study cohort was 8.0 years (range, 4.3-22.4), with a median weight of 19.9 kg (8.4-88.7) and a median height of 120.6 cm (86.7-178.8). All but one patient were younger than 18 years of age. Figure 1 shows the BMI distribution of the

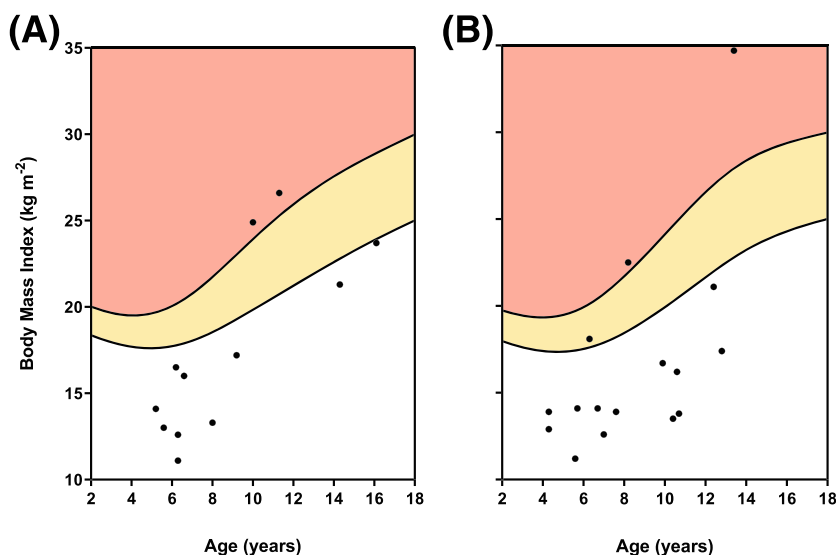


**FIGURE 1** BMI distribution for male (A) and female (B) patients in the study population (black circles). Black lines are locally weighted scatterplot smoothing curves through international cut-off points for BMI for overweight (lower curve) and obesity (upper curve) proposed by Cole *et al.*<sup>32</sup> The yellow area indicates overweight, whereas patients in the red area are considered obese. One patient (male, 22.4 years of age, BMI =  $23.9 \text{ kg m}^{-2}$ ) is not included in this graph, since overweight and obesity in adulthood is determined differently, ie, BMI greater than 25 and  $30 \text{ kg m}^{-2}$ , respectively

population, including overweight and obesity classification based on age and sex specific cut-off points for BMI as proposed by Cole *et al.*<sup>32</sup> This study population included one overweight and four patients in the obese group. In comparison to the National Health and Nutrition Examination Survey (NHANES) data,<sup>33</sup> patients tended to have a short stature and be underweight, with a BMI on the lower end of the spectrum in both males and females (Figure 2).

### 3.2 | Population PK modelling

A two-compartment model with zero-order infusion adequately described the PK profile of busulfan after intravenous infusion. A proportional error model provided an adequate fit, while a combined proportional and additive residual error model did not perform significantly better. Allometric scaling of TBM significantly improved the model fit ( $\Delta\text{OFV} = -169$ ,  $P < 0.001$ ). The power exponents of TBM were estimated to be 0.863 (95% confidence interval (CI): 0.722-1.00) for clearance (CL) and intercompartmental clearance (Q), and 0.931 (95% CI: 0.812-1.05) for volume of distribution of the central ( $V_1$ ) and peripheral compartment ( $V_2$ ). The 95% CIs included the theoretical power exponents (0.75 for clearance and 1.0 for volume)

which were proposed by Holford and Anderson.<sup>22</sup> Therefore, the fixed power exponents of 0.75 and 1.0 were used for allometric scaling of clearance (CL and Q) and volume of distribution ( $V_1$  and  $V_2$ ), respectively. This model was defined as the base model. Of other body mass describing covariates examined, FFM provided the best model fit ( $\Delta\text{OFV} = -28.3$ ,  $P < 0.001$ ). Using IBM gave similar results, since IBM values approximated those of FFM, especially in obese patients. PK parameter estimates were standardized to  $\text{FFM}_{\text{std}} = 56.1$  kg, which was calculated by a standard adult height of 176 cm and weight of 70 kg.<sup>34</sup> Estimated exponents of FFM were 0.984 (95% CI: 0.852-1.12) on CL and Q, and 1.06 (95% CI: 0.994-1.13) on  $V_1$  and  $V_2$ , suggesting a linear relationship between FFM and the PK parameters. Hence, both the exponents for clearances and volumes of distribution were fixed to 1.0. The inter-individual variability (IIV) for Q and  $V_2$  were fixed to 0, since they could not be estimated probably due to small sample size. No other covariates were found to be significant. The FFM model was selected as the final model. The population PK parameter estimates in the final model are summarized in Table 2.

Figure 3 shows the goodness-of-fit plots for the final model. The model adequately predicts the concentration ( $R^2 = 0.91$  and 0.99 for population- and individual-predicted vs observed busulfan

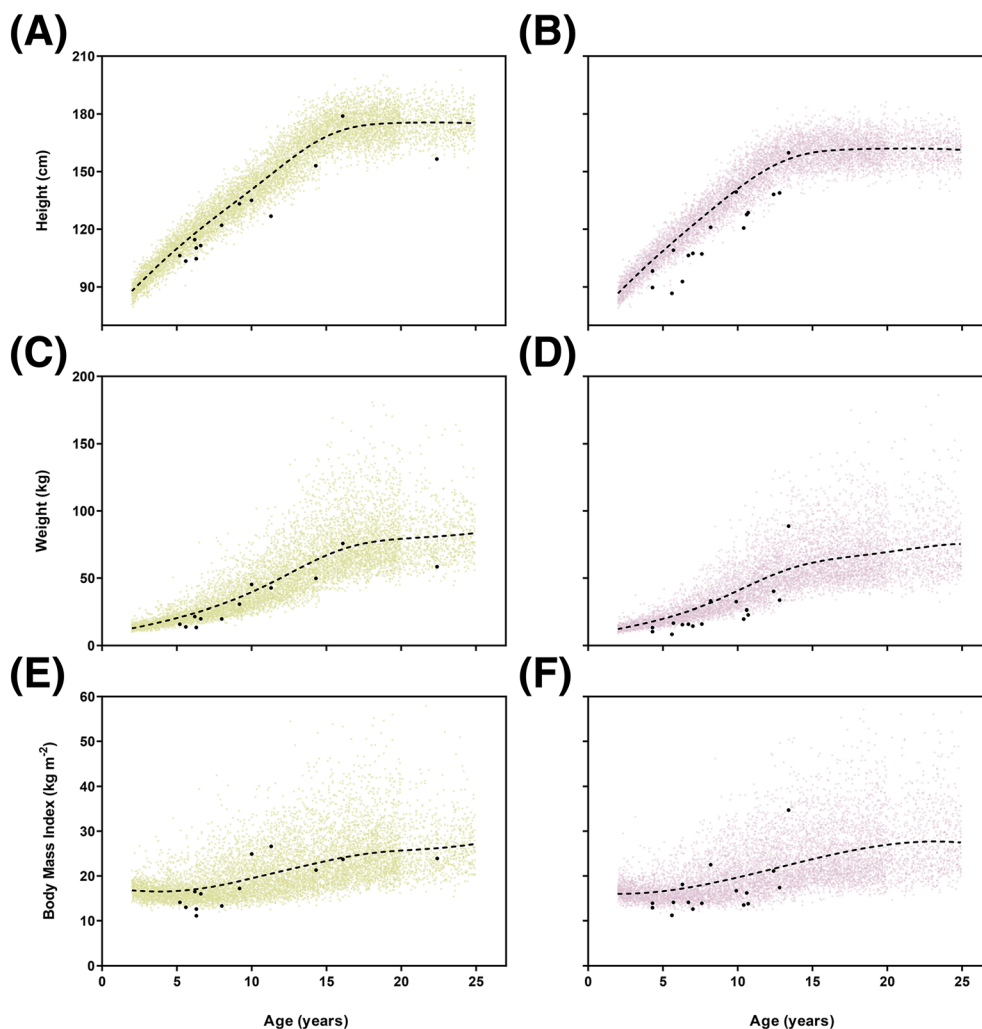


**FIGURE 2** Age versus height (A, B), weight (C, D) and BMI (E, F) for male (left column) and female (right column) patients (black circles) plotted with the NHANES data (yellow and purple shading for men and women, respectively), executed by Centers for Disease Control and Prevention (CDC) over the years 2005-2014. The dashed line is a locally weighted scatterplot smoothing curve through the NHANES data

**TABLE 2** Parameter estimates for the final population PK model and bootstrap analysis

| Parameter                                   | Final model |         |               | Bootstrap analysis |        |       |
|---|-------------|---------|---------------|--------------------|--------|-------|
|   | Estimate    | RSE (%) | Shrinkage (%) | Median             | 95% CI |       |
|   |             |         |               |                    | Lower  | Upper |
| CL (L h <sup>-1</sup> 70 kg <sup>-1</sup> ) | 12.6        | 3       | ...           | 12.6               | 11.8   | 13.4  |
| V <sub>1</sub> (L 70 kg <sup>-1</sup> )     | 36.4        | 7       | ...           | 36.2               | 31.6   | 41.2  |
| Q (L h <sup>-1</sup> 70 kg <sup>-1</sup> )  | 11.8        | 37      | ...           | 12.4               | 3.25   | 20.3  |
| V <sub>2</sub> (L 70 kg <sup>-1</sup> )     | 7.73        | 28      | ...           | 7.73               | 3.48   | 12.0  |
| IIV (CV%)                                   |             |         |               |                    |        |       |
| IIV for CL                                  | 16.2        | 33      | -1            | 16.0               | 10.3   | 20.8  |
| IIV for V <sub>1</sub>                      | 11.8        | 25      | 4             | 11.9               | 8.98   | 15.4  |
| IIV for Q                                   | ...         | ...     | ...           | ...                | ...    | ...   |
| IIV for V <sub>2</sub>                      | ...         | ...     | ...           | ...                | ...    | ...   |
| Residual variability (CV%)                  |             |         |               |                    |        |       |
| Proportional error                          | 4.09        | 41      | 15            | 4.03               | 2.77   | 5.59  |

Note. Parameter estimates are standardized for an adult male with 70 kg of body weight and 176 cm of height (FFM<sub>std</sub> = 56.1 kg).

Abbreviations: CI, confidence interval; CL, clearance; CV, coefficient of variation; IIV, interindividual variability; Q, intercompartmental clearance; RSE, relative standard error; V<sub>1</sub>, central compartment; V<sub>2</sub>, peripheral compartment.

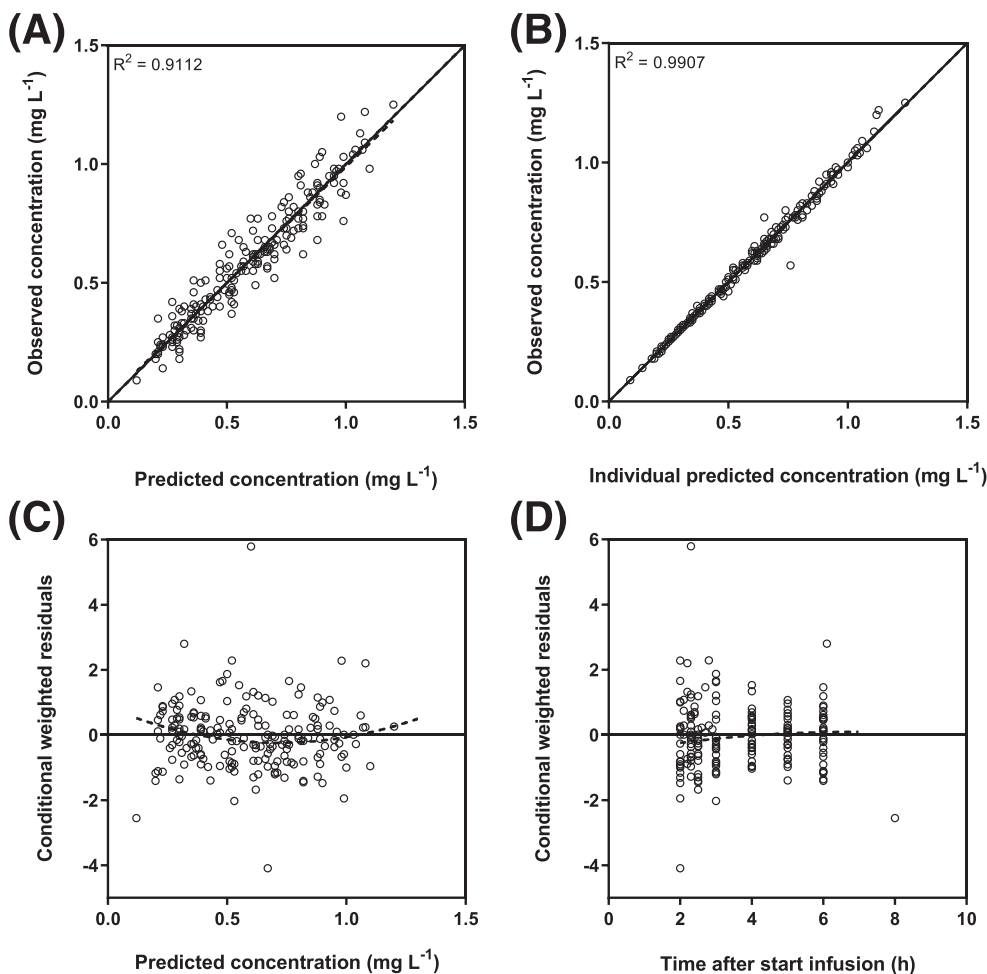


**FIGURE 3** Goodness-of-fit plots for the final PK model. Population-predicted (A) and individual-predicted (B) busulfan concentrations vs observed concentrations (solid line, line of identity; dashed line, linear regression; open circles, observed data). Conditional weighted residuals (CWRES) vs (C) population-predicted busulfan concentration and (D) time after start of the infusion (solid line, line of identity; dashed line, second-order polynomial; open circles, observed data)

concentration, respectively). Bootstrap analysis indicated the stability of the final model (Table 2). The simulated concentrations by pcVPC (Figure 4) presented a good agreement between the observed and simulated concentrations. Figure 5 shows plasma concentration time

profiles for underweight (defined as BMI < fifth percentile of NHANES data), normal weight (defined as BMI ≈ 50th percentile of NHANES data), and obese male and female patients. Population-based estimation of plasma concentration time curves was

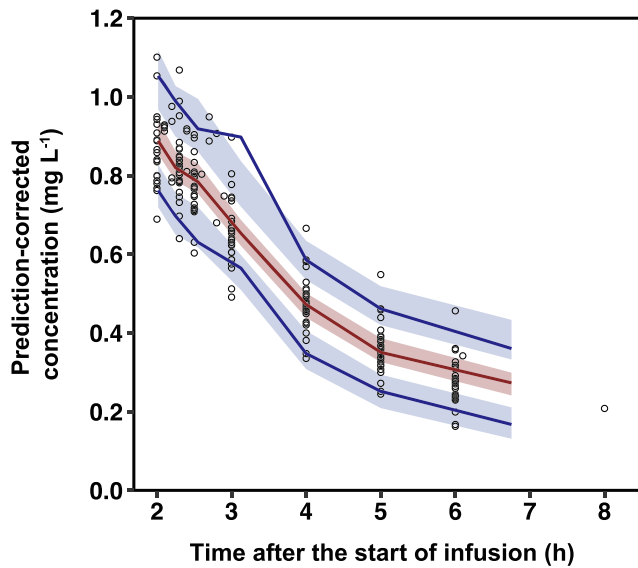


**FIGURE 4** Prediction-corrected visual predictive check (pcVCP) for the final model of busulfan. Open circles represent observed concentration. The solid red line represents the median of the observed concentration, and the shaded red area represents a simulation-based 95% CI for the median. The solid blue lines represent the 95th and 5th percentiles of the observed data, and the simulation-based 95% CIs for the 95th and 5th percentiles are shown as the shaded blue areas

satisfactory in normal weighted patients and was slightly less precise in underweight and obese patients, but seemed to be unbiased (ie, no trend of under- or overprediction in under- or overweighted patients).

### 3.3 | Estimated steady-state concentrations following TBM- and FFM-based doses

Calculated  $C_{ss}$  values following the initial dose of 0.6 or 0.8 mg kg<sup>-1</sup> TBM, as well as estimated  $C_{ss}$  values following simulated doses of 0.6 mg kg<sup>-1</sup> TBM, 0.6 mg kg<sup>-1</sup> FFM and 0.8 mg kg<sup>-1</sup> FFM, plotted against patients' BMI, are depicted in Figure 6 (panels A through D, respectively). Following the initial dose of 0.6 or 0.8 mg kg<sup>-1</sup> TBM, there seemed to be a trend of higher  $C_{ss}$  if the patient was more overweight (slope of linear regression line significantly different from zero;  $P = 0.0019$ ). Notably, three out of four obese patients received the higher 0.8 mg kg<sup>-1</sup> TBM dose. In the simulated scenario in which all patients received the same 0.6 mg kg<sup>-1</sup> TBM dose, the trend endured nonetheless (slope different from zero;  $P < 0.001$ ). Additionally, non-obese patients achieved a mean (standard deviation (SD))  $C_{ss}$  of 0.265 (0.0402) mg L<sup>-1</sup>, whereas obese patients were exposed to significantly higher concentrations (0.345 (0.0742) mg L<sup>-1</sup>;  $P = 0.0091$ ) after receiving the simulated 0.6 mg kg<sup>-1</sup> TBM dose. Conversely, simulated FFM-based dosing regimens of 0.6 and 0.8 mg kg<sup>-1</sup> FFM achieved

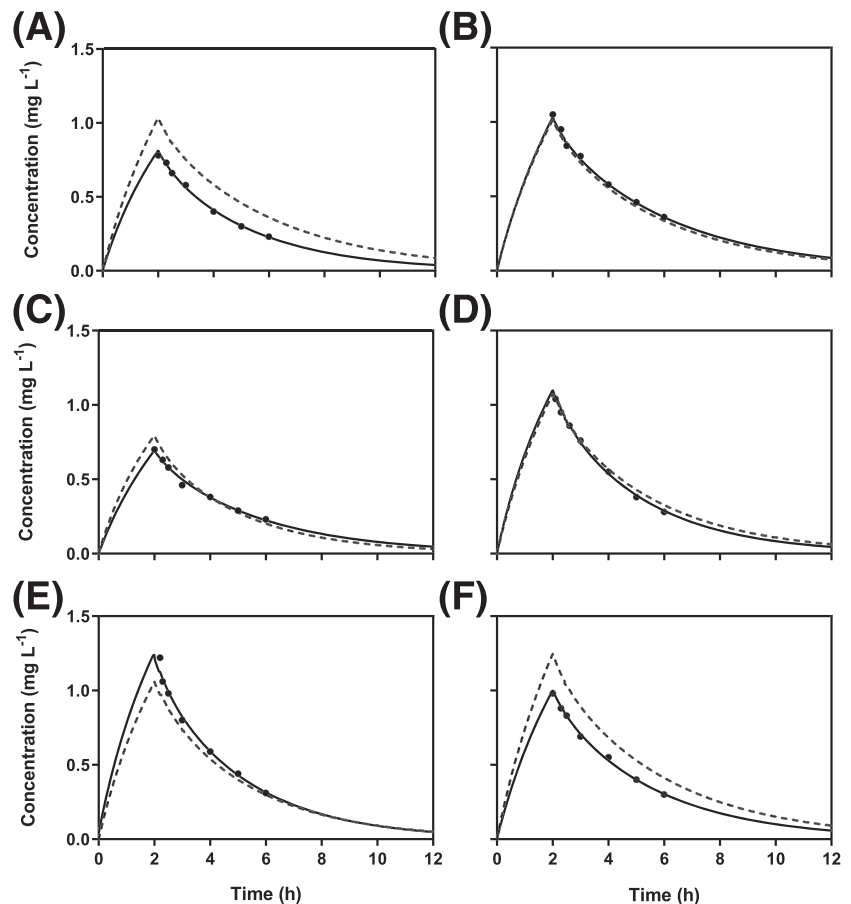


**FIGURE 5** Plasma concentration-time profiles of intravenous busulfan for underweight (A, B), normal weight (C, D), and obese (E, F) patients following the first dose. The left column represents male patients, female patients are represented by the right column. The dashed line is the population-based prediction, black circles are observed data, and the solid line is the individually predicted fit

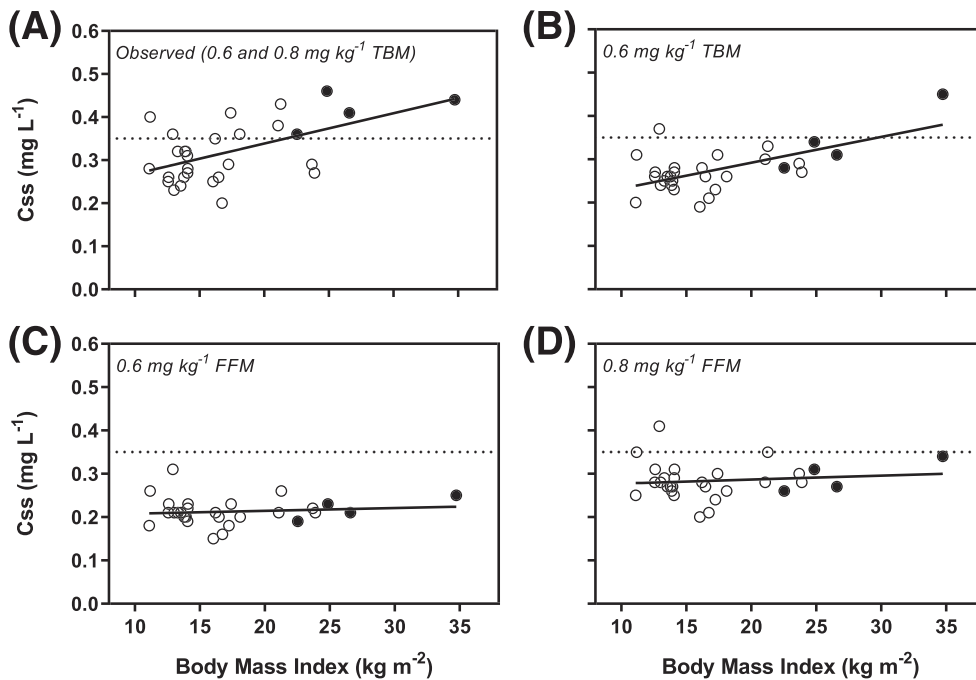


**FIGURE 6** Individual steady-state concentrations ( $C_{ss}$ ) following the initial dose (A, 0.6 and 0.8 mg kg<sup>-1</sup> TBM) and simulated doses (B, 0.6 mg kg<sup>-1</sup> TBM; C, 0.6 mg kg<sup>-1</sup> FFM; D, 0.8 mg kg<sup>-1</sup> FFM) plotted against the body mass index (BMI) of the patient. Open circles represent non-obese patients and obese patients are represented by black circles. The dotted line represents the proposed upper  $C_{ss}$  limit (target  $\leq 0.35$  mg L<sup>-1</sup>). The solid line represents the linear regression line

steady  $C_{ss}$  across the BMI spectrum (slope not different from zero;  $P = 0.57$  and  $P = 0.54$ , respectively).

Estimated  $C_{ss}$  values following simulated doses of 0.6, 0.8, 1.0 and 1.2 mg kg<sup>-1</sup> TBM and FFM are shown in Figure 7. The mean (interquartile range, IQR)  $C_{ss}$  was 0.28 (0.25-0.30), 0.37 (0.33-0.41), 0.46 (0.41-0.51) and 0.55 (0.49-0.61) mg L<sup>-1</sup> for the 0.6, 0.8, 1.0 and 1.2 mg kg<sup>-1</sup> TBM dose, respectively. The IQR was narrower across FFM-based doses, with mean (IQR)  $C_{ss}$  of 0.21 (0.20-0.23), 0.28 (0.26-0.30), 0.35 (0.33-0.38) and 0.43 (0.39-0.45) mg L<sup>-1</sup> for the 0.6, 0.8, 1.0 and 1.2 mg kg<sup>-1</sup> FFM dose, respectively. Obese patients attained  $C_{ss}$  at the higher end of the distribution when receiving a TBM-based dose. FFM-based dosing, in contrast, resulted in similar  $C_{ss}$  predictions between obese and non-obese patients.

## 4 | DISCUSSION

This is the first study to characterize PK of busulfan in paediatric patients with FA through population PK analysis. Individual busulfan PK profiles were predicted adequately in FA patients by the population PK model, which was developed using FFM as the most important size descriptor. With the developed model, consecutive busulfan doses that are part of the conditioning regimen can be tailored with greater precision. Regarding PK characteristics in FA paediatric patients, size-normalized busulfan clearance and volume of distribution estimates were not essentially different from previously published values in non-FA paediatric patients (Figure 8).<sup>13-17</sup> Our estimated busulfan clearance (mean (SD); 12.6 (2.04) L h<sup>-1</sup> per 56.1 kg FFM) is the highest among previously reported values, and 12.8% higher than the value reported by McCune *et al.* (11.4 (2.45) L h<sup>-1</sup> per 62 kg NFM).<sup>17</sup> The FFM of 56.1 kg and NFM of 62 kg both

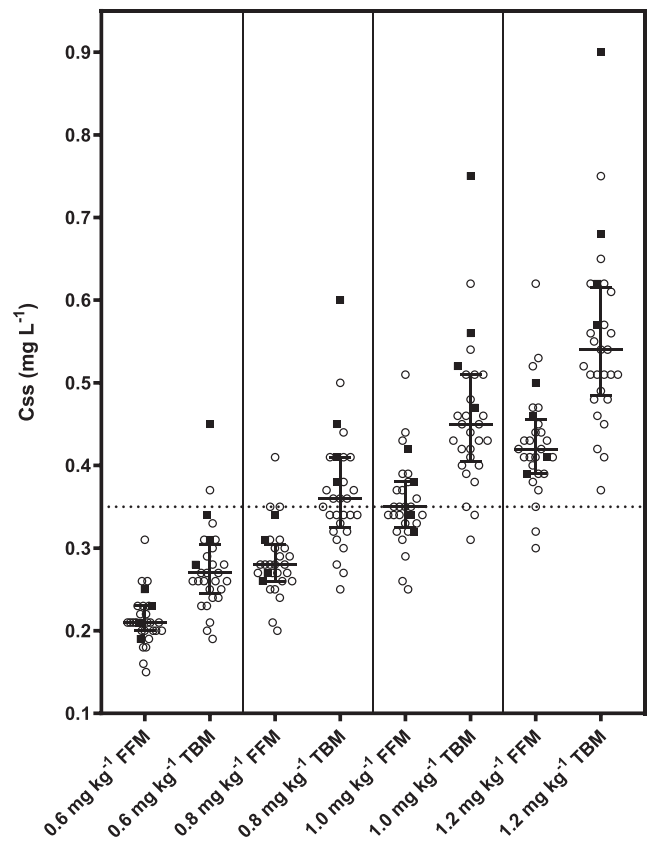


**FIGURE 7** Individual steady-state concentration ( $C_{ss}$ ) following simulated FFM- and TBM-based doses. Open circles represent non-obese patients and obese patients are represented by black squares. Solid horizontal lines represent median with interquartile range (IQR) per dosing regimen. Solid vertical lines mark 0.6, 0.8, 1.0 and 1.2 mg kg<sup>-1</sup> dosing scenarios. The dotted line represents the proposed upper  $C_{ss}$  limit (target  $\leq 0.35$  mg L<sup>-1</sup>)

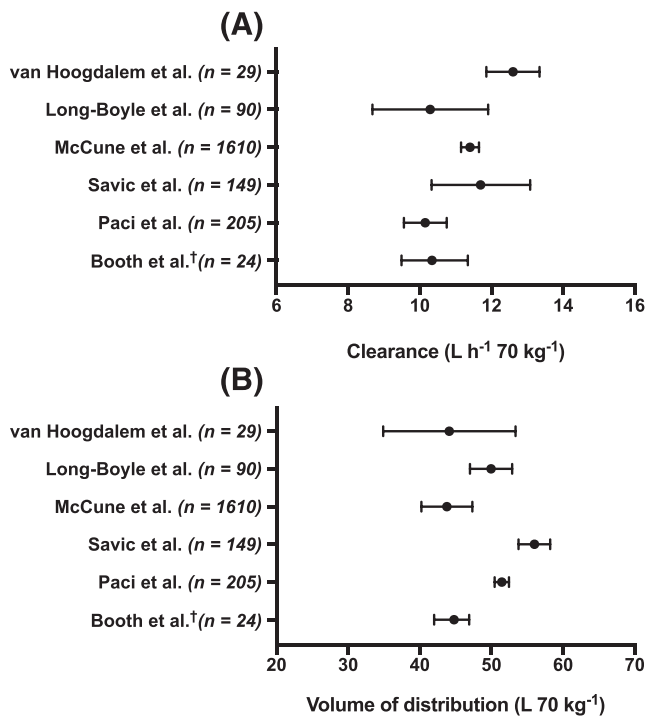


**FIGURE 8** Estimated clearance (A) and volume of distribution (B) related population pharmacokinetic parameters in FA patients compared to reported values in non-FA paediatric patients.<sup>13-17</sup> All values, which were often expressed corresponding to the median weight of the population, were allometrically scaled to a total body weight of 70 kg, using the theoretical power exponents of 0.75 and 1.0 for clearance and volume, respectively. Both one- and two-compartment models have been reported. Since one-compartment models inherently include only one volume of distribution ( $V_d$ ), this value was compared to the sum of the estimated volumes for the central and peripheral compartment ( $V_{ss}$ ) in two-compartment models. Black circles represent the estimated value, with whiskers showing the 95% confidence interval of the mean estimate, unless stated otherwise.

†Whiskers show the 90% confidence interval

correspond to a TBM of 70 kg. This difference in clearance is not considered clinically relevant. Our study with a sample size of 29 patients had more than 90% power to detect a 20% difference (two-sided) in clearance with a type I error of 0.05 using the large study population of McCune *et al.* as the control group.

Patient's gender and several clinical laboratory test results were applied to clearance as potential covariates; however, they did not show any significant improvement of the model fit, which is consistent with other reports in non-FA patients.<sup>14,15</sup> Regarding the clearance of busulfan, the primary pathway is conjugation with glutathione in the liver by glutathione S-transferase (GST), with the GSTA1-1 isoform being the most active form of GST.<sup>35</sup> As hepatic conjugation capacity decreases in case of liver injury, this could affect the elimination of busulfan. Liver transaminases, ALT and AST, were elevated (ie, above the 97th percentile of the healthy paediatric reference value for that sex and age<sup>36</sup>) in around half of the subjects, indicating potential liver damage in these patients. Yet these enzymes were not found to be significant covariates, which might indicate that liver damage in

terms of ALT or AST elevation does not essentially affect the conjugation of busulfan in our population. However, no conclusions can be drawn due to the small sample size and the relatively small range of transaminase values.

Age has been found to be a significant covariate associated with busulfan PK in non-FA paediatric patients,<sup>16,17,19</sup> while this was not observed in our analysis. This might be explained by the difference in age in the study cohort, since the youngest patient in our study was 4.3 years of age, while other trials included patients as young as 0.1 years. Size-standardized busulfan clearance reaches 95% of the adult value at 2.5 year of age.<sup>17</sup> Hence, this could explain why no age effect was observed in our study cohort.

In this study, multiple body mass descriptors were examined to assess the effects of differences in body size on busulfan PK in paediatric FA patients. FFM proved to be the most informative predictive covariate and was implemented in the population PK model. Using NFM gave the same model fit, since  $Ffat$  was estimated to be virtually 0 for both elimination processes and physiological volumes (ie,  $Ffat = 0.005$  and  $0.028$  for clearance and volume, respectively). It should be noted, however, that the deviation of  $Ffat$  from 0 could not be adequately estimated due to small sample size and large interindividual variability. The estimated values for  $Ffat$  are not in accordance with what has been observed before by McCune *et al.* since they found  $Ffat = 0.509$  and  $0.203$  for clearance and volume, respectively.<sup>17</sup> This difference might be explained by the fact that FFM was predicted by another approach that had been established in adults, but not in children. If we used the same approach to estimate FFM, we observed  $Ffat = 0.150$  and  $0.507$  for clearance and volume, respectively. Moreover, this resulted in a worse fit of the model ( $\Delta OFV = +10.91$ ,  $P < 0.001$ ) and fixing  $Ffat$  values to 0 further decreased the fitness ( $\Delta OFV = +22.58$ ,  $P < 0.001$ ), compared to our final model. However, as stated earlier,  $Ffat$  values could not be estimated adequately and are confounded by the allometric model assumption, thus cannot be compared directly to those of McCune *et al.*

The proposed model has a few limitations. The formula that was used to calculate the FFM in children is based on patients with an age range of 3-29 years. Moreover, as noted earlier, busulfan clearance is different in neonates and small infants, most likely due to GST ontogeny.<sup>37</sup> Clinicians should therefore exercise caution when applying this model to children under the age of 3 years. However, median time to develop marrow failure in patients with FA is 7 years of age.<sup>2</sup> Hence, that scenario is not expected to occur commonly in clinical practice. Furthermore, there were not enough data to determine the interindividual variability (IIV) for the peripheral compartment ( $V_2$ ) and intercompartmental clearance ( $Q$ ), so these values were fixed to 0 in this study.

As weight increased in overweight patients, the  $C_{ss}$  tended to be higher in comparison to non-obese patients. However, three out of four obese patients received the higher busulfan dose of  $0.8 \text{ mg kg}^{-1}$  TBM. To determine whether being in the higher dosed group of the study or obesity was the cause of the higher  $C_{ss}$ , steady-state concentrations were estimated in the simulated scenario in which all patients

received the same 0.6 mg kg<sup>-1</sup> TBM dose. Still, obese patients were predicted to be exposed to higher concentrations of busulfan than non-obese patients ( $P = 0.0091$ ). This could be explained by the tendency of busulfan to distribute over total body water.<sup>38</sup> Obese patients have more adipose tissue that is unlikely to contribute to the volume of distribution of busulfan due to its hydrophilic properties (ie,  $\log P = -0.36^{39}$ ), although total body mass is taken into account when dosing the patient. That could also explain why, if patients received an FFM-based dose, steady-state concentrations did not increase if the patient was more overweight.

Individual  $C_{ss}$  estimates for FFM-based dosing regimens show a narrower IQR than TBM-based dosing regimens. This indicates that dosing FA patients based on their FFM could reduce variability in busulfan exposure and increase target  $C_{ss}$  attainment rate. In obese patients, TBM-based dosing attained  $C_{ss}$  at the higher end of the population distribution (eg, all obese patients above the proposed target of  $C_{ss} \leq 0.35$  mg L<sup>-1</sup> following 0.8 mg kg<sup>-1</sup> TBM). This was not observed with an FFM-based dosing approach (eg, no obese patients above target following 0.8 mg kg<sup>-1</sup> FFM), and this is thus expected to reduce the risk of overdosing obese patients compared to the currently established TBM-based dosing strategy. We emphasize, however, that the current study is limited in sample size and that the results are derived from modelling and simulation. The findings must be further substantiated prospectively in a larger study.

## 5 | CONCLUSION

A population PK model of busulfan in paediatric FA patients that incorporates FFM was developed that will allow improved prediction of busulfan exposure. FA patients were found to have similar size-normalized busulfan PK as non-FA patients. Conventional dosing, which is based on an amount of busulfan per kg TBM, attains a higher  $C_{ss}$  if the patient is more overweight, increasing the risk of overdosing. Dosing based on FFM is expected to improve target exposure, especially in obese patients, since the achieved  $C_{ss}$  is predicted to be unbiased over a wide range of BMI values.

### ACKNOWLEDGEMENTS

We gratefully acknowledge the contributions of Nieko Punt, MSc, for guiding the development of the pharmacokinetic model of busulfan in FA patients. In addition, the insights provided by Min Dong, PhD, comparing the FA demographic data to the NHANES data, were essential for the evaluation of our data.

### COMPETING INTERESTS

There are no competing interests to declare.

### CONTRIBUTORS

M.W.vH. wrote the draft manuscript. All authors reviewed and edited the manuscript. M.W.vH. and T.M. developed the model and analysed the data. M.W.vH., C.E., T.F., T.M. and A.A.V. contributed to the interpretation of the results. P.A.M. provided key clinical insights. P.A.M.

and A.A.V. conceived the presented research and were in charge of overall direction and planning. A.A.V. supervised the project.

### DATA AVAILABILITY STATEMENT

The data that support the findings of this study are available on request from the PI. The data are not publicly available due to ongoing studies.

### ORCID

Matthijs W. van Hoogdalem  <https://orcid.org/0000-0002-8979-8797>

Chie Emoto  <https://orcid.org/0000-0002-8933-0254>

Tsuyoshi Fukuda  <https://orcid.org/0000-0002-0477-3102>

Tomoyuki Mizuno  <https://orcid.org/0000-0002-8471-9826>

Alexander A. Vinks  <https://orcid.org/0000-0003-4224-2967>

### REFERENCES

- Joenje H, Patel KJ. The emerging genetic and molecular basis of Fanconi anaemia. *Nat Rev Genet.* 2001;2(6):446-457.
- Auerbach AD. Fanconi anemia and its diagnosis. *Mutat Res.* 2009;668(1-2):4-10.
- Gluckman E, Auerbach A, Horowitz M, et al. Bone marrow transplantation for Fanconi anemia. *Blood.* 1995;86(7):2856-2862.
- Grochow LB, Jones RJ, Brundrett RB, et al. Pharmacokinetics of busulfan: correlation with veno-occlusive disease in patients undergoing bone marrow transplantation. *Cancer Chemother Pharmacol.* 1989;25(1):55-61.
- Andersson BS, Thall PF, Madden T, et al. Busulfan systemic exposure relative to regimen-related toxicity and acute graft-versus-host disease: defining a therapeutic window for i.v. BuCy2 in chronic myelogenous leukemia. *Biol Blood Marrow Transplant.* 2002;8(9):477-485.
- Slattery JT, Clift RA, Buckner CD, et al. Marrow transplantation for chronic myeloid leukemia: the influence of plasma busulfan levels on the outcome of transplantation. *Blood.* 1997;89(8):3055-3060.
- Slattery JT, Sanders JE, Buckner CD, et al. Graft-rejection and toxicity following bone marrow transplantation in relation to busulfan pharmacokinetics. *Bone Marrow Transplant.* 1995;16(1):31-42.
- Gluckman E, Devergie A, Schaison G, et al. Bone marrow transplantation in Fanconi anaemia. *Br J Haematol.* 1980;45(4):557-564.
- Walden H, Deans AJ. The Fanconi anemia DNA repair pathway: structural and functional insights into a complex disorder. *Annu Rev Biophys.* 2014;43:257-278.
- Mehta PA, Emoto C, Fukuda T, et al. Busulfan pharmacokinetics and precision dosing: are patients with Fanconi anemia different? *Biol Blood Marrow Transplant.* 2019 ;25(12):2416-2421.
- Nguyen L, Fuller D, Lennon S, Leger F, Puozzo C. I.V. busulfan in pediatric patients: a novel dosing to improve safety/efficacy for hematopoietic progenitor cell transplantation recipients. *Bone Marrow Transplant.* 2004;33(10):979-987.
- Trame MN, Bergstrand M, Karlsson MO, Boos J, Hempel G. Population pharmacokinetics of busulfan in children: increased evidence for body surface area and allometric body weight dosing of busulfan in children. *Clin Cancer Res.* 2011;17(21):6867-6877.
- Booth BP, Rahman A, Dagher R, et al. Population pharmacokinetic-based dosing of intravenous busulfan in pediatric patients. *J Clin Pharmacol.* 2007;47(1):101-111.
- Paci A, Vassal G, Moshous D, et al. Pharmacokinetic behavior and appraisal of intravenous busulfan dosing in infants and older children: the results of a population pharmacokinetic study from a large pediatric cohort undergoing hematopoietic stem-cell transplantation. *Ther Drug Monit.* 2012;34(2):198-208.

15. Long-Boyle JR, Savic R, Yan S, et al. Population pharmacokinetics of busulfan in pediatric and young adult patients undergoing hematopoietic cell transplant: a model-based dosing algorithm for personalized therapy and implementation into routine clinical use. *Ther Drug Monit.* 2015;37(2):236-245.
16. Savic RM, Cowan MJ, Dvorak CC, et al. Effect of weight and maturation on busulfan clearance in infants and small children undergoing hematopoietic cell transplantation. *Biol Blood Marrow Transplant.* 2013;19(11):1608-1614.
17. McCune JS, Bemer MJ, Barrett JS, Baker KS, Gamis AS, Holford NHG. Busulfan in infant to adult hematopoietic cell transplant recipients: a population pharmacokinetic model for initial and Bayesian dose personalization. *Am J Clin Cancer Res.* 2014;20(3):754-763.
18. Bartelink IH, van Kesteren C, Boelens JJ, et al. Predictive performance of a busulfan pharmacokinetic model in children and young adults. *Ther Drug Monit.* 2012;34(5):574-583.
19. Neely M, Philippe M, Rushing T, et al. Accurately achieving target busulfan exposure in children and adolescents with very limited sampling and the BestDose software. *Ther Drug Monit.* 2016;38(3):332-342.
20. Mehta PA, Davies SM, Leemhuis T, et al. Radiation-free, alternative-donor HCT for Fanconi anemia patients: results from a prospective multi-institutional study. *Blood.* 2017;129(16):2308-2315.
21. Slattery JT, Rislis LJ. Therapeutic monitoring of busulfan in hematopoietic stem cell transplantation. *Ther Drug Monit.* 1998;20(5):543-549.
22. Holford NHG, Anderson BJ. Allometric size: the scientific theory and extension to normal fat mass. *Eur J Pharm Sci.* 2017;109S:S59-S64.
23. Green B, Duffull SB. What is the best size descriptor to use for pharmacokinetic studies in the obese? *Br J Clin Pharmacol.* 2004;58(2):119-133.
24. Janmahasatian S, Duffull SB, Ash S, Ward LC, Byrne NM, Green B. Quantification of lean bodyweight. *Clin Pharmacokinet.* 2005;44(10):1051-1065.
25. Al-Sallami HS, Goulding A, Grant A, Taylor R, Holford N, Duffull SB. Prediction of fat-free mass in children. *Clin Pharmacokinet.* 2015;54(11):1169-1178.
26. Kendrick JG, Carr RR, Ensom MHH. Pharmacokinetics and drug dosing in obese children. *J Pediatr Pharmacol Ther.* 2010;15(2):94-109.
27. Traub SL, Kichen L. Estimating ideal body mass in children. *Am J Hosp Pharm.* 1983;40(1):107-110.
28. Devine BJ. Gentamicin therapy. *Drug Intell Clin Pharm.* 1974;8:650-655.
29. Ette EI. Stability and performance of a population pharmacokinetic model. *J Clin Pharmacol.* 1997;37(6):486-495.
30. Bergstrand M, Hooker AC, Wallin JE, Karlsson MO. Prediction-corrected visual predictive checks for diagnosing nonlinear mixed-effects models. *AAPS J.* 2011;13(2):143-151.
31. Palmer J, McCune JS, Perales MA, et al. Personalizing busulfan-based conditioning: considerations from the American Society for Blood and Marrow Transplantation Practice Guidelines Committee. *Biol Blood Marrow Transplant.* 2016;22(11):1915-1925.
32. Cole TJ, Bellizzi MC, Flegal KM, Dietz WH. Establishing a standard definition for child overweight and obesity worldwide: international survey. *BMJ.* 2000;320(7244):1240-1243.
33. Centers for Disease Control and Prevention (CDC). National Health and Nutrition Examination Survey 2005-2014. <https://wwwn.cdc.gov/nchs/nhanes/>. Accessed May 4, 2017.
34. Anderson BJ, Holford NH. Mechanism-based concepts of size and maturity in pharmacokinetics. *Annu Rev Pharmacol Toxicol.* 2008;48:303-332.
35. Czerwinski M, Gibbs JP, Slattery JT. Busulfan conjugation by glutathione S-transferases alpha, mu, and pi. *Drug Metab Dispos.* 1996;24(9):1015-1019.
36. Bussler S, Vogel M, Pietzner D, et al. New pediatric percentiles of liver enzyme serum levels (alanine aminotransferase, aspartate aminotransferase,  $\gamma$ -glutamyltransferase): effects of age, sex, body mass index, and pubertal stage. *Hepatology.* 2018;68(4):1319-1330.
37. ten Brink MH, van Bavel T, Swen JJ, et al. Effect of genetic variants GSTA1 and CYP3A1 and age on busulfan clearance in pediatric patients undergoing hematopoietic stem cell transplantation. *Pharmacogenomics.* 2013;14(14):1683-1690.
38. Hassan M, Ljungman P, Bolme P, et al. Busulfan bioavailability. *Blood.* 1994;84(7):2144-2150.
39. Hassan M, Ehrsson H, Wallin I, Eksborg S. Pharmacokinetic and metabolic studies of busulfan in rat plasma and brain. *Eur J Drug Metab Pharmacokinet.* 1988;13(4):301-305.

## SUPPORTING INFORMATION

Additional supporting information may be found online in the Supporting Information section at the end of this article.

**How to cite this article:** van Hoogdalem MW, Emoto C, Fukuda T, Mizuno T, Mehta PA, Vinks AA. Population pharmacokinetic modelling of busulfan and the influence of body composition in paediatric Fanconi anaemia patients. *Br J Clin Pharmacol.* 2020;86:933-943. <https://doi.org/10.1111/bcp.14202>